THE JOURNAL OF BIOLOGICAL CHEMISTRY
Vol. 273, No. 43, Issue of October 23, pp. 28247–28252, 1998

Printed in U.S.A.

The *H19* Transcript Is Associated with Polysomes and May Regulate *IGF2* Expression in *trans**

(Received for publication, May 20, 1998, and in revised form, July 9, 1998)

Yi-Ming Li‡, Gary Franklin‡, Heng-Mi Cui‡, Kristian Svensson‡, Xiao-Bing He‡, Gail Adam‡, Rolf Ohlsson‡, and Susan Pfeifer‡§¶

From the ‡Department of Animal Development & Genetics, Uppsala University, Norbyvägen 18A, S-752 36 Uppsala, Sweden and the §Department of Pediatrics, Uppsala University Hospital, S-751 85 Uppsala, Sweden

The imprinted *H19* gene produces a fully processed transcript that does not exhibit any conserved open reading frame between mouse and man. Although transcriptional control elements associated with the mouse *H19* locus have been shown to control the neighboring *Igf2* gene in *cis,* the prevailing view is that the cytoplasmic *H19* transcript does not display any function. In contrast to earlier reports, we show here that the *H19* transcript is associated with polysomes in a variety of cell types, in both mouse and man. A possible *trans*-function of the *H19* gene is suggested by a reciprocal correlation in *trans* between cytoplasmic *H19* and *IGF2* mRNA levels, as well as *IGF2* mRNA translatability. We discuss these results in terms of their challenge to the prevailing dogma on the function of the enigmatic *H19* gene, as well as with respect to the ontogeny of the Beckwith-Wiedemann syndrome, and propose that the human *H19* gene is an antagonist of *IGF2* expressivity in *trans*.

The *H19* gene, which was first identified a decade ago, has been suggested to belong to the category of polymerase II-driven genes that do not code for a protein product (1). Although the processed and polyadenylated transcript is highly conserved between mouse and man, it does not display a conserved open reading frame (2). Moreover, the mouse *H19* transcript, which is localized in the cytoplasm, has been reported to be excluded from the polysomal fraction and to be unable to be translated *in vitro* (2). The only indication so far that the human *H19* RNA may have any role derives from the observation that an *H19* expression vector rescues the normal phenotype of rhabdomyosarcoma cells (3). This result would, however, appear to be at odds with the lack of a documented increased incidence of cancer in *H19*-deficient mice (4). Moreover, *H19* expression is maintained at high levels in some human tumors and has been proposed to be selected for during the generation of choriocarcinoma (5). No consistent role (if any) has been established, therefore, for *H19* in *trans*.

Both *H19* and the insulin-like growth factor gene-2 (*IGF2*), which are close physical neighbors on chromosome 7 in mouse and on chromosome 11 in humans (6), were among the first genes to be identified as being genomically imprinted (7, 8). The generation of deletion mutants in the mouse has shown that the imprinting status of *Igf2* and *H19* is coordinated such that the deletion of *H19* and a 10-kilobase upstream region up-regulates maternal *Igf2* when the deleted region is maternally inherited (4, 9). Conversely, a deletion of the endodermal-specific *H19* enhancers has shown that they are vital for the activity of paternally derived *Igf2*, at least in some cell types, when the deleted enhancer region is inherited paternally (10). It appears, therefore, that the region within and/or flanking the mouse *H19* gene can regulate the allele-specific expression of *Igf2* in *cis*.

The observations that many human tumors do not express *H19,* but express both parental *IGF2* alleles, has prompted suggestions that the human *H19* gene or its flanking sequences may also control the activity of *IGF2* in *cis* (11, 12). Such notions have not, however, been substantiated at the cellular level. Indeed, it has been shown by examination at the cellular level that *H19* can be biallelically expressed in a subpopulation of human placental cells that expresses *IGF2* monoallelically (13). It has also been shown that the generation of Wilms' tumors involves a mosaic *IGF2* imprinting status that does not correlate with the expression of *H19* at the individual cellular level (14). Collectively, these data, although circumstantial, are not supportive with respect to a *cis* function of the human *H19* gene.

Here we report that, in contrast to previous claims, the *H19* transcript is associated with polysomes in a variety of cell types in both mouse and man. *H19* expression appears to directly or indirectly modulate the cytoplasmic levels of *IGF2* mRNAs without being genetically linked to the expressed *IGF2* allele. We submit that the human *H19* gene is an antagonist to *IGF2* in *trans*.

EXPERIMENTAL PROCEDURES

Cell Samples and Extraction of Nucleic Acid—The Wilms' tumor was collected at the Uppsala University hospital. Routinely processed formalin-fixed, paraffin-embedded tissues were used for *in situ* hybridizations. DNA was extracted from snap-frozen tissues and from peripheral leukocytes, as has been described previously (13). The mouse embryos, at 17 days postconception, were crosses between *Mus mus musculus* and *Mus mus domesticus*. The JEG-3 cell line was maintained as has been described (15). Pactamycin (a kind gift of Pharmacia-Upjohn) was administered to JEG-3 cells for 3.5 h before harvesting and used at a concentration of either 2.0 or 6.9×10^{-6} M without any detectable difference in the effect. Genomic DNA and total cellular RNA were prepared according to routine protocols (13).

Sucrose Gradient Analysis—Postmitochondrial supernatants of both mouse embryos and cultured tumor cells were prepared according to Brannan *et al.* (2). Supernatants without added EDTA were layered onto 10.6 ml of 10–50% sucrose gradient containing 50 mM Tris-HCl (pH 7.5), 50 mM KCl, 10 mM $MgCl_2$, and 15 units of RNasin/ml. The supernatant with added EDTA (30 mM final concentration) was layered onto a 10.6-ml 10–50% sucrose gradient containing 50 mM Tris-HCl (pH 7.5), 50 mM KCl, 30 mM EDTA. The gradients were centrifuged in an LKB 2331 ultracentrifuge with a 40T768 rotor at 38,000 rpm for 1.5 or

* This work was supported by the Swedish Cancer Research Foundation (CF), The Swedish Pediatric Cancer Foundation (BCF), the Natural Science Research Council (NFR), the Wenner-Gren Foundation, and the von Hofsten Foundation. The costs of publication of this article were defrayed in part by the payment of page charges. This article must therefore be hereby marked "*advertisement*" in accordance with 18 U.S.C. Section 1734 solely to indicate this fact.

¶ To whom correspondence should be addressed. E-mail: Susan.Pfeifer@Devbiol.uu.se.

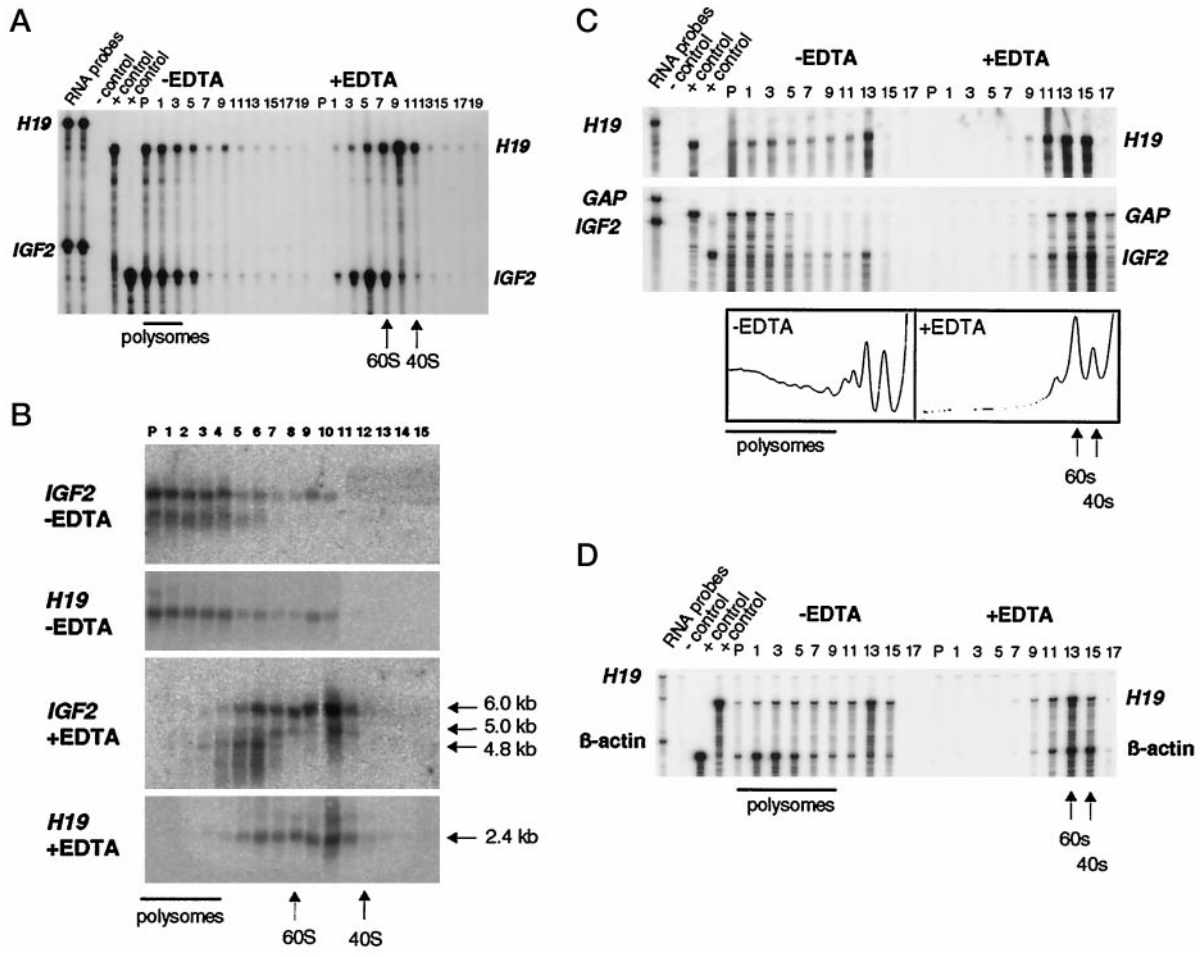

FIG. 1. **Sedimentation properties of *H19* RNA in sucrose gradients.** Postmitochondrial lysates were analyzed on sucrose gradients as described under "Experimental Procedures." RNA was extracted from gradient fractions and subjected to RNase protection (*A*, *C,* and *D*) or Northern blot hybridization (*B*) analysis, as indicated. *A-C*, distribution of *H19* and *IGF2* transcripts in JEG-3 cells. *D*, sedimentation of *H19* and β-actin transcripts in liver cells of a mouse fetus (17 days postconception) in sucrose gradients. Sucrose density gradients analyzed in (*A* and *B*) and (*C* and *D*) were centrifuged for 4 and 1 h, respectively. The UV-recorded polysomes are displayed in *panel C*. The positions of the 40 S and 60 S subunits were determined by agarose gel analyses of extracted RNA of aliquotted sucrose density gradient fractions. The position of the polysomes in the gradients is inferred from UV-recorded sucrose density gradients, as exemplified in *panel C*. The amplitude of the *right-hand panel* (*+EDTA*) is reduced to allow comparison with the *left-hand panel* (*−EDTA*). The images are scanned x-ray films with the exception for *panel B*, which is derived from a Fuji phosphoimager file. The *−control lane* indicates that yeast tRNA was used to assess any unspecific band pattern, whereas the *+control lane* shows the specific bands that could be obtained when examining the input RNA with each individual labeled RNA probe.

6 h, as indicated in the legend to Fig. 1. Following division into 18–20 fractions, RNA was phenol-extracted from 100-μl aliquots and analyzed by Northern blot, RNase protection assay, and RT-PCR.[1]

*Probes—Dde*I-linearized human *H19* cDNA cloned in Bluescript (a kind gift from Dr. Wolf Reik, Babraham, Cambridge, UK) was used to generate an antisense riboprobe (253 bases; T7 polymerase). A 558-base pair *Hin*fI-*Pst*I human *IGF2* cDNA insert, cloned in pGem-3 and encompassing exon 7 to the 5′-region of exon 9, was cut with *Xho*I and used as the template for generation of an antisense riboprobe (145 bases; SP6 polymerase) (16). A 756-base pair antisense *H19* RNA probe (17) was used to detect mouse *H19* transcripts.

Northern Blot Hybridization and RNase Protection Analysis—Northern blot hybridization analysis on 1% agarose gels was performed as described (18). RNase protection analysis was performed using the RPA II™ ribonuclease protection assay kit (Ambion).

Analysis of Allele-specific IGF2 Transcripts—The overall functional *IGF2* imprinting status was determined by thermocyclic amplification of cDNA, produced by priming of *IGF2* mRNA, and by diagnostic digestion with *Apa*I as has been described (19, 20) with the following exception. To ensure a linear amplification of low abundance *IGF2* cDNAs in the sucrose gradient analyses, the oligo primers were 5′-labeled and the number of cycles were reduced to 25. This approach was verified by mixing experiments (not shown) as has been described (21). The resulting PCR products were analyzed on 8% polyacrylamide-urea sequencing gels, as has been described (21).

Allelic expression patterns at the cellular level were analyzed by allele-specific *in situ* hybridization as has been reported (13, 14). Regular *in situ* hybridization analysis of *IGF2* and *H19* expression was performed as has been described (13). Both approaches used serial 5-μm sections from formaldehyde-fixed and paraffin-embedded tissues according to routine procedures. Following hybridization, the slides were dipped in NTB2 (Kodak) emulsion, developed, and counterstained in Mayer's hematoxylin before mounting.

RESULTS

The H19 Transcript Co-sediments with Polysomes—In initial attempts to identify any ribonucleoprotein particles containing human *H19* RNA, we investigated the distribution of *H19* RNA in the cytoplasm of JEG-3 choriocarcinoma cells. Our approaches included sucrose density gradient centrifugation analysis of postmitochondrial cell lysates. Fig. 1*A* shows an RNase protection analysis which documents that *H19* RNA distributes along a 10–50% sucrose gradient, with a peak that appeared to partially overlap with polysomes containing *IGF2* mRNAs. In EDTA-treated samples, the collapse of the polysome to generate ribosomal subunits appears to be accompanied by a similar shift of the *H19* RNA-protein complexes to the

[1] The abbreviations used are: RT-PCR, reverse transcription-polymerase chain reaction; BWS, Beckwith-Wiedemann syndrome.

upper portion of the sucrose gradient. To examine the extent of sedimentation overlap of *H19* RNA-protein complexes with polysomes containing the different types of *IGF2* mRNA transcripts derived from the three major promoters, we repeated the experiment and analyzed the sucrose gradient fractions by Northern blot analysis. Fig. 1*B* shows that there is an extensive similarity in the distribution of *H19* RNA with the promoter 3-derived 6.0-kilobase *IGF2* transcript. Because this similarity extends to the samples treated with EDTA, we reasoned that *H19* might be associated with polysomes of a size similar to those containing *IGF2* mRNA.

Because such a high proportion of the RNA-protein complexes pelleted in our sucrose gradient analyses, we were prompted to resolve the pelleted *H19* transcripts. We repeated the sucrose gradient analyses, therefore, using a significantly shorter centrifugation time. Fig. 1*C* shows that the resolution of the distribution of the *H19* transcript in sucrose gradient analyses of JEG-3 cells is improved with such a change in the protocol. The previous notion that the *H19* transcript co-sediments with polysomes is reinforced by these results. All of these observations have been reproduced numerous times with very similar or identical results.

Given that it has been previously argued that mouse *H19* RNA is not associated with polysomes (2), we subjected *H19* transcripts expressed in mouse fetal liver to a polysome analysis, using the shorter centrifugation periods described above. The results show that the distribution of *H19* RNA partially overlapped with the polysomal marker, β-actin mRNA (Fig. 1*D*). Both types of transcripts appear to exist in polysomal and non-polysomal pools. As was the case for the human *H19* RNA, the mouse *H19* RNA (and the β-actin mRNA) was shifted to the lighter portion of the sucrose density gradient in the presence of EDTA. We have performed these experiments according to the protocol of Brannan *et. al*. (2) with the exception of the cycloheximide treatment. Because cycloheximide would stabilize the polysomes and potentially yield larger polysomes than in untreated animals, it is possible that such polysomes would pellet quantitatively during centrifugation, perhaps explaining why *H19* RNA association to polysomes has gone unnoticed (2).

It was still possible that the sedimentation properties of the *H19* transcript were fortuitously similar to the polysome profile of control transcripts, such as GAP and β-actin mRNAs. To resolve this issue, we treated JEG-3 cells with pactamycin, which is an inhibitor of initiation of mRNA translation. Fig. 2 shows that the shift in sedimentation properties of the control GAP mRNA in pactamycin-treated cells is accompanied by a similar, but less dramatic, shift in the sedimentation of both the *H19* and *IGF2* transcripts. We conclude that *H19* is associated with polysomes, at least in human cells. The reason for the less pronounced difference in pactamycin-sensitivity for the *IGF2* and *H19* transcripts, when compared with the GAP mRNA, is not known. One possible explanation is that the elongation of the *IGF2* and *H19* transcripts is attenuated. This would be expected to yield polysomes that are less sensitive to pactamycin treatment, as has been demonstrated for polysomes containing the HSP70 mRNA (22).

Absence of H19 Transcripts Correlates with Increased Cytoplasmic Levels of IGF2 mRNA in a Wilms' Tumor—We have previously documented a Wilms' tumor that is unique in the sense that it expresses *IGF2* and *H19* at high levels in almost identical patterns and displays a postneoplastic loss of *IGF2* imprinting, where only a subpopulation of the tumor cells express both parental alleles, as determined by allele-specific *in situ* hybridization (Fig. 3*A*) (14). Fig. 3*B* shows a summary of these results: where subpopulations of cells with no *H19* expression but monoallelic *IGF2* expression are marked *red*, and

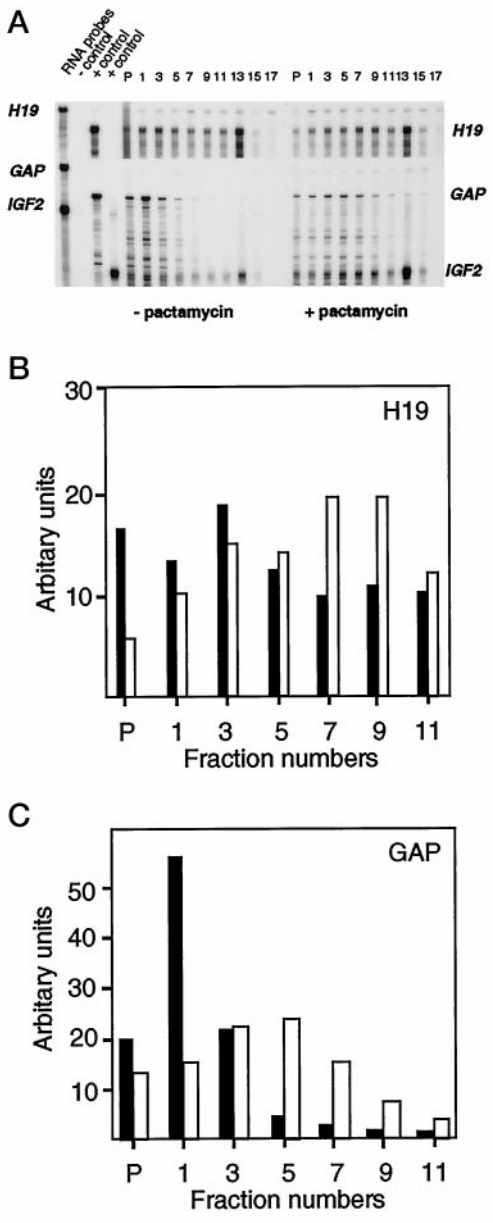

FIG. 2. **The sedimentation property of the *H19* transcript is pactamycin-sensitive.** Postmitochondrial lysates of JEG-3 cells, control, and pactamycin-treated were analyzed on sucrose gradients as described under "Experimental Procedures." RNA was extracted from every second fraction and subjected to RNase protection (*A*). The analysis of the sedimentation properties of the *H19* transcript was performed separate from the analysis of the *GAP* and *IGF2* mRNAs. The *H19*- (*B*) and *GAP*- (*C*) specific protected bands were quantitated by PhosphorImager analysis. The filled and unfilled staples display relative levels of transcripts in control and pactamycin-treated cells, respectively.

cells with no *H19* expression and biallelic *IGF2* expression are marked *green*. Magnified views of these areas can be seen in Cui *et al.* (14). A closer look at the *IGF2* expression levels revealed that the hybridization signal was 2–3-fold higher in the *H19*-negative cells when compared with the neighboring *H19*-positive cells (Fig. 3*B*). This observation could be documented in each of the *H19*-negative areas, suggesting an inverse correlation between *H19* expression and cytoplasmic levels of *IGF2* mRNA.

H19 Expression Correlates Inversely with Translatability of IGF2 mRNAs in a Wilms' Tumor—We next addressed whether or not the pattern of *H19* expression correlates with a difference in the polysome profile of *IGF2* mRNAs. This approach

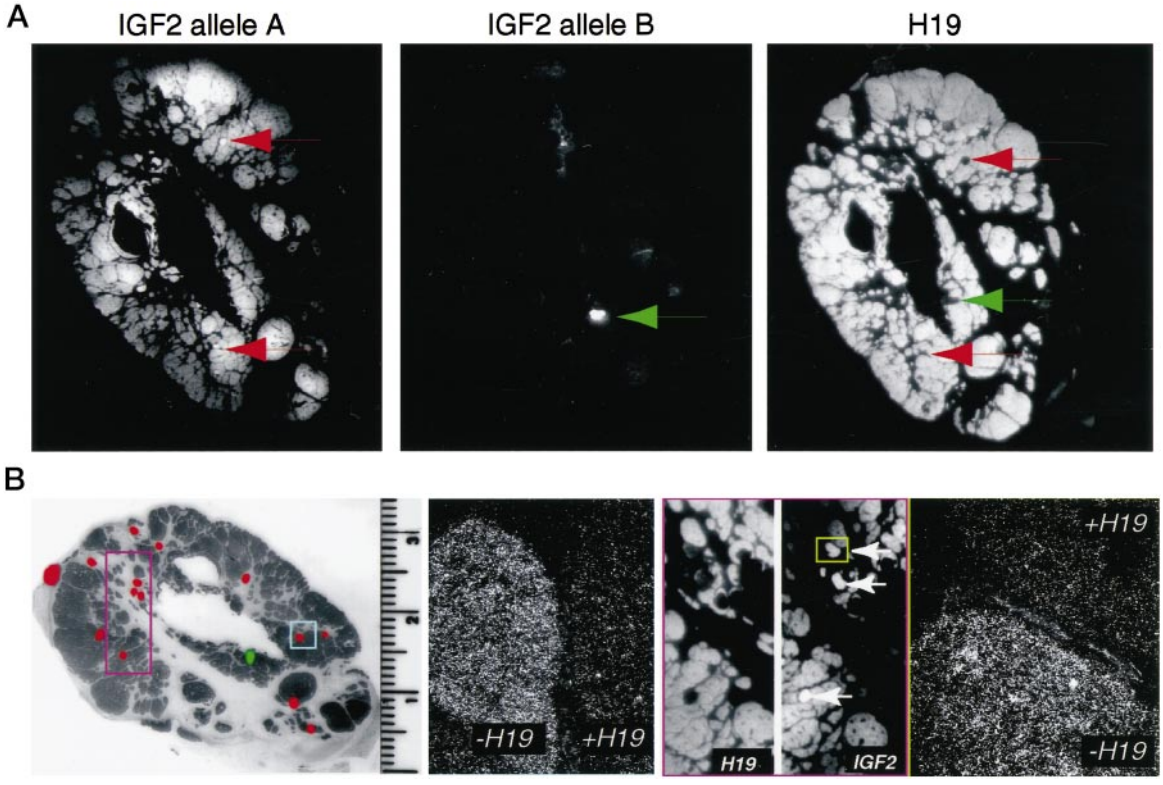

FIG. 3. **Inverse correlation of *IGF2* and *H19* transcripts in a Wilms' tumor as analyzed by *in situ* hybridization.** *Panel A*, shows x-ray images (inverted in the computer using Adobe Photoshop 4.0) of allelic *IGF2* expression patterns, as determined by oligo DNA-based *in situ* hybridization analysis (*frames* marked *IGF2 allele A* and B) (14). The *frame* marked as *H19* is the result of an antisense riboprobe hybridized to a section immediately adjacent to those hybridized to allele-specific *IGF2* probes. *Red arrows* pinpoint just a few of the cell populations that do not express *H19* but expresses increased levels of the allele A of the *IGF2* gene. *Green arrows* identify the subpopulation of cells that is *H19*-negative and expresses *IGF2* biallelically. *Panel B* summarizes these results and shows relationships between *H19* and *IGF2* expression patterns in closer detail. The *left-most frame* provides a bright-field overview of cells that lack *H19* expression but express *IGF2* monoallelically (*red*) and cells that lack *H19* expression and express *IGF2* biallelically (*green*). All the other *frames* of *panel B* are dark-field views to show *IGF2* or *H19* expression patterns in adjacent sections, as indicated in the figure. The magnified images are color-coded to identify the boxed areas. Magnifications are (2.2-fold (*red-lila-encoded image* magnified in *panel B*) and 44-fold (*yellow* and *blue-encoded images* magnified in *panel B*). *Images* in *panel A* are magnified 1.3-fold. The brightfield view of the *left-most frame* of *panel B* shows actual size.

was made possible by the strategy outlined in Fig. 4, where the parental alleles (A and B) are distinguishable by a sequence polymorphism. The generally silent allele B of *IGF2* was only expressed in *H19*-negative cells, whereas the majority of the tumor cells expressed only the normally active allele A in *H19*-positive cells. If *H19* expression modifies the translatability of *IGF2* mRNAs, we would predict that the over-all sedimentation properties of transcripts derived from alleles A and B would differ in a sucrose gradient analysis.

The postmitochondrial cell lysate of the Wilms' tumor was subjected, therefore, to a sucrose density gradient fractionation. Fig. 5*A* shows that, in contrast to the specimens analyzed in Fig. 1, the sedimentation properties of the various *IGF2* mRNP complexes in the sucrose gradients were refractory to EDTA treatment, as examined by Northern blot hybridization. This result suggests that the bulk of *IGF2* mRNAs was poorly translated in this Wilms' tumor. We next examined whether or not the presence or absence of *H19* transcripts correlated with the sedimentation properties of *IGF2* transcripts, as outlined above. To this end, *IGF2* mRNA, which was extracted from every second sucrose gradient fraction, was subjected to reverse transcription. Using labeled primers to thermocyclically amplify a fragment encompassing a diagnostic *Apa*I polymorphic site, the cDNA was digested with *Apa*I to allow discrimination of allelic origin. Fig. 5*B* shows that the *IGF2* transcripts derived from allele A, which is predominantly expressed in *H19*-positive cells, are associated with gradient fractions, which suggest that they are poorly translated. This result

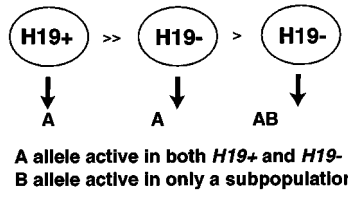

FIG. 4. **The rationale for examining the effect of *H19* expression on the association of *IGF2* RNA with polysomes in the Wilms' tumor.**

agrees well with the conclusion from the Northern blot hybridization analysis of the samples from the same sucrose gradient. Conversely, the *IGF2* transcripts derived from the allele B (exclusively expressed in *H19*-negative cells) generally sediment as larger complexes than transcripts derived from allele A. Upon the addition of EDTA, the relative distribution of these transcripts is shifted to fractions containing nontranslated *IGF2* mRNA.

Because it has been hypothesized that mitotic crossing-overs can switch the parental epigenotype during Wilms' tumorigenesis (23), we could not formally exclude the possibility that the epigenotype of allele B would be maternal in the tumor and paternal in the normal kidney. If so, the suggested overrepresentation of allele B-derived *IGF2* transcripts in the polysome fraction might simply reflect contamination of stroma cells expressing allele B at low or undetectable levels (see Fig. 3). A thermocyclic amplification analysis of reverse transcribed

mRNA, extracted from both normal and tumor compartments, revealed that allele A can be found to be preferentially active in both instances (Fig. 6). Given the more than 50-fold lower expression of *IGF2* in the normal cells, it appears clear that *IGF2* transcripts derived from allele B are highly unlikely to result from contamination by stroma and are, therefore, expressed only in tumor cells.

DISCUSSION

A function for *H19* in *trans* has been disputed because a previous study claims that the *H19* transcript is not associated with polysomes and does not produce a protein in the mouse (2). In addition, the lack of a reported increased incidence of cancer in *H19*-deficient mice (4) would appear to question a link to the suggested tumor suppressor function of human *H19* in *trans*. On the other hand, the *H19* knock out data does not rule out that an *H19 trans*-function is redundant and/or that a removal of an *H19* function in *trans* contributes to the overgrowth phenotype of *H19*-deficient conceptuses. In addition, it is possible that human *H19* has acquired a *trans*-function that is absent or has been lost in the mouse during evolution. Moreover, a recent transgenic study has strongly argued against the possibility that the mouse *H19* gene represses the transcription of *Igf2* in *cis,* by means of its own expression (24). We have, therefore, reexamined a putative role for the *H19* transcript in humans.

First, we document that in contrast to previous reports, *H19* mRNA co-sediments with polysomes in a variety of cell types, in both mouse and man. In cell cultures, this sedimentation is sensitive to pactamycin, which is an inhibitor of initiation of mRNA translation. This observation would seem to support a previous observation that the human *H19* transcript is translatable *in vitro* and has an open reading frame that could formally encode a protein of 26 kDa (25). Second, by both direct and indirect lines of evidence, we were able to document that the cytoplasmic levels of *H19* transcripts inversely correlated with cytoplasmic levels of *IGF2* in a Wilms' tumor. Because the parental *H19* alleles were identical with respect to a number of polymorphic markers, we have been unable to trace the parental origin of the expressed allele. On the other hand, because

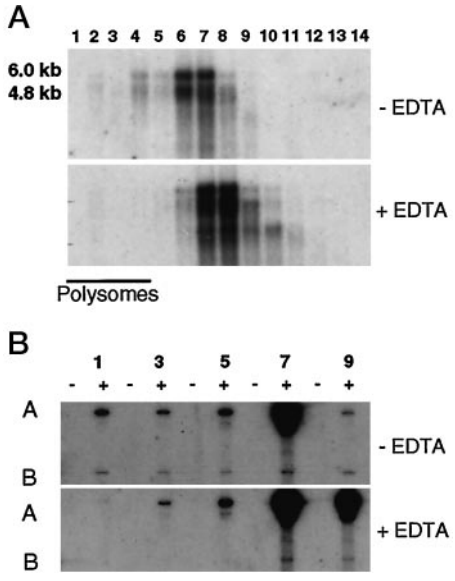

FIG. 5. **Parent of origin-dependent sedimentation properties of Wilms' tumor-derived *IGF2* mRNAs in sucrose gradients.** *A*, Northern blot analysis of *IGF2* mRNA species extracted from every second fraction. *B*, selected fractions of the sucrose gradient of *panel A* were subjected to RT-PCR analysis to examine allelic origin of *IGF2* transcripts. *Panels A* and *B* denote the *Apa*I noncutting and cutting alleles, respectively. − and + denote minus and plus reverse transcriptase, respectively.

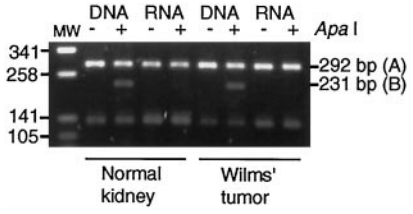

FIG. 6. **Analysis of allelic expression pattern of *IGF2* in the normal kidney tissue and Wilm's tumor of the same patient.** The analysis was carried out by *Apa*I digestion of genomic PCR products (DNA) and RT-PCR products (RNA). The molecular weight (*MW*) marker lane displays *Sau3A* I/*Taq*I-restricted pUC 19 DNA (Stratagene). The extra band, migrating as a 140-base pair fragment, represents a PCR artifact.

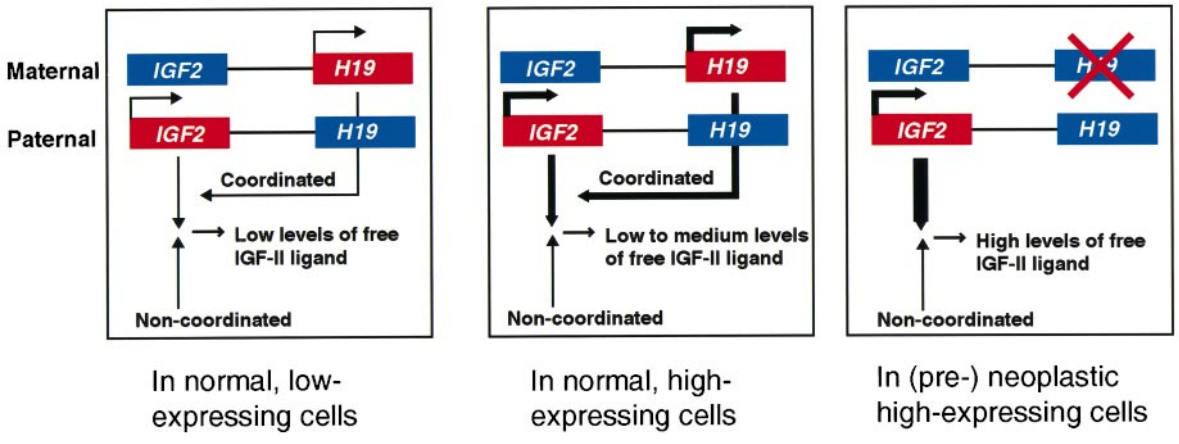

FIG. 7. **A model of the postulated *H19*-specific control loop.** Whereas the *H19*-specific control would be coordinated with *IGF2* activity, other levels of controls, represented by IGF-binding proteins for example, may be uncoordinated. In the normal context with cells displaying low levels of *IGF2* mRNAs, the noncoordinated controls would be expected to successfully prevent production of high levels of IGF-II peptide. The coordinated control, represented by *H19* transcripts, will be of minor importance because the levels and pattern of *H19* expression closely follows those of *IGF2* (27). By the same token, increased activity of the *IGF2* gene will be followed by increased activity of the *H19* gene. In this scenario, the coordinated *H19* control would gain importance in direct proportion to the inability of the uncoordinated controls to deal with abnormal levels of *IGF2* activity. If the *H19* function is abnormally silenced in a situation with high levels of *IGF2* transcripts, as has been documented in numerous contexts (31), this report suggests that production of the IGF-II peptide will increase abnormally to contribute to overgrowth syndrome syndromes, such as the Beckwith-Wiedemann syndrome, and neoplasia (outlined in the *right-most panel*). This model may be valid only in the absence of prominent translational suppression of *IGF2* mRNAs.

absence of *H19* transcripts correlates both with increased levels of cytoplasmic transcripts derived from one allele and with increased translatability of transcripts derived from the other allele, we argue that one or both of these effects can be attributed to an *H19* function in *trans*. Collectively, the data support the notion that *H19* modifies *IGF2* mRNA cytoplasmic levels and, potentially, polysome association in *trans*.

The observations of this report provide yet another glimpse into the complex regulation of the function of *IGF2*. This involves multiple steps of controls from gene dosage, differential promoter usage, splicing patterns, translational control(s) to postsecretory attenuation of *IGF2* function by IGF-binding proteins (26). Whereas some of the cytoplasmic and extra-cellular levels of control appear to be uncoordinated with *IGF2* expression levels, the expression of *H19*, and hence the antagonistic function of *H19* in *trans*, is expected to be coordinated (27). This allows us to formulate a model in which *H19* serves to prevent overshoot of *IGF2* expression in *trans*. In this model, an increase in *H19* expression would accompany an increase in *IGF2* expression because their expression patterns are coordinated (10, 27) (Fig. 7). This coordination would be of particular importance in cases where the high levels of *IGF2* expression could be expected to saturate the uncoordinated types of negative cytoplasmic and/or extracellular controls, such as IGF-binding proteins. In practice, this would mean that the higher the levels of *IGF2* expression, the more important the *H19* regulatory pathway would become. According to this model, a loss of the *H19* function in *trans* would be expected to be a key event in cells expressing high levels of *IGF2* mRNAs, resulting in a significant increase of free IGF-II ligand. Our model would highlight the consequences of losing the *H19* function in *trans* when *IGF2* is overexpressed. In a parallel study, we have been able to show that this loss of *H19* expression is an early event which may predispose for Wilms' tumors (14). Another interesting case is the previous documentation that *IGF2* could not be genetically linked with a familial form of BWS (28), despite the close link between BWS and *IGF2* (29, 30). The possibility that *H19* can be the direct culprit in this cancer-predisposing disease, at least in some instances, and that the role of *IGF2* may be more indirect would appear to be compatible with the proposed model.

Our observations are consistent with the possibility that the human *H19* gene modifies the expression of *IGF2* in *trans*. These data may have an impact in our understanding of human diseases, such as BWS, and allows us to further penetrate the nature of disease-associated (epi)genetic abnormalities.

Acknowledgment—We are grateful to Helena Malmikumpu for excellent technical assistance.

REFERENCES

1. Tilghman, S., Bartolomei, M., Webber, A., Brunkow, M., Saam, J., Leighton, P., Pfeifer, K., and Zemel, S. (1993) *Cold Spring Harbor Symp. Quant. Biol.* **58,** 287–295
2. Brannan, C., Dees, E., Ingram, R., and Tilghman, S. (1990) *Mol. Cell. Biol.* **10,** 28–36
3. Hao, Y., Crenshaw, T., Moulton, T., Newcomb, E., and Tycko, B. (1993) *Nature* **365,** 764–767
4. Leighton, P. A., Ingram, R. S., Eggenschwiler, J., Efstratiadis, A., and Tilghman, S. M. (1995) *Nature* **375,** 34–39
5. Rachmilewitz, J., Elkin, M., Rosensaft, J., Gelman-Kohan, Z., Ariel, I., Lustig, O., Schneider, T., Goshen, R., Biran, H., De Groot, N., and Hochberg, A. (1995) *Oncogene* **11,** 863–870
6. Zemel, S., Bartolomei, M., and Tilghman, S. (1992) *Nat. Genet.* **2,** 61–65
7. Bartolomei, M., Zemel, S., and Tilghman, S. (1991) *Nature* **351,** 153–155
8. DeChiara, T., Robertson, E., and Efstratiadis, A. (1991) *Cell* **64,** 849–859
9. Ripoche, M., Kress, C., Poirier, F., and Dandolo, L. (1997) *Genes Dev.* **11,** 1596–1604
10. Leighton, P., Saam, J., Ingram, R., Stewart, C., and Tilghman, S. (1995) *Genes Dev.* **9,** 2079–2089
11. Tycko, B. (1994) *Am. J. Path.* **144,** 431–443
12. Feinberg, A., Kalikin, L., Johnson, L., and Thompson, J. (1994) *Cold Spring Harbor Symp. Quant. Biol.* **59,** 357–364
13. Adam, G., Cui, H., Miller, S., Flam, F., and Ohlsson, R. (1996) *Development* **122,** 839–847
14. Cui, H., Hedborg, F., He, L., Nordenskjöld, A., Sandstedt, P.-O. S., and Ohlsson, R. (1997) *Cancer Res.* **57,** 4469–4473
15. Franklin, G., Donovan, M., Adam, G., Holmgren, L., Specht, A., Pfeifer-Ohlsson, S., and Ohlsson, R. (1991) *EMBO J.* **10,** 1365–1373
16. Ekström, T. J., Cui, H., Li, X., and Ohlsson, R. (1995) *Development* **121,** 309–316
17. Walsh, C., Glaser, A., Fundele, R., Ferguson-Smith, A., Barton, S., Surani, M. A., and Ohlsson, R. (1994) *Mech. Dev.* **46,** 55–62
18. Ohlsson, R., Holmgren, L., Glaser, A., Szpecht, A., and Pfeifer-Ohlsson, S. (1989) *EMBO J.* **8,** 1993–1999
19. Ogawa, O., Eccles, M., Szeto, J., McNoe, L., Yun, K., Maw, M., Smith, P., and Reeve, A. (1993) *Nature* **362,** 749–751
20. Ekström, T. J., Cui, H., Nyström, A., Rutanen, E.-M., and Ohlsson, R. (1995) *Mol. Reprod. Dev.* **41,** 177–183
21. He, L., Cui, H., Walsh, C., Mattsson, R., Lin, W., Anneren, G., Pfeifer-Ohlsson, S., and Ohlsson, R. (1998) *Oncogene* **16,** 113–119
22. Theodorakis, N., Banerji, S., and Morimoto, R. (1988) *J. Biol. Chem.* **263,** 14579–14585
23. Cote, G. B. (1995) in *Genomic Imprinting: Causes and Consequences* (Ohlsson, R., Hall, K., and Ritzen, M., eds) pp. 252–263, Cambridge University Press, Cambridge
24. Webber, A., Ingram, R., Levorse, J., and Tilghman, S. (1998) *Nature* **391,** 711–715
25. Joubel, A., Curgy, J.-J., Pelczar, H., Begue, A., Lagrou, C., Stehelin, D., and Coll, J. (1996) *Cell. Mol. Biol.* **42,** 1159–1172
26. Stewart, C. E., and Rotwein, P. (1996) *Physiol. Rev.* **76,** 1005–1026
27. Ohlsson, R., Hedborg, F., Holmgren, L., Walsh, C., and Ekström, T. J. (1994) *Development* **120,** 361–368
28. Nyström, A., Hedborg, F., and Ohlsson, R. (1994) *Eur. J. Pediatr.* **153,** 574–580
29. Reeve, A. E. (1996) *Med. Pediatr. Oncol.* **27,** 470–475
30. Hedborg, F., Holmgren, L., Sandstedt, B., and Ohlsson, R. (1994) *Am. J. Pathol.* **145,** 802–817
31. Tycko, B. (1998) in *Genomic Imprinting: An Interdisciplinary Approach* (Ohlsson, R., ed), Springer, Heidelberg, in press

The *H19* Transcript Is Associated with Polysomes and May Regulate *IGF2* Expression in *trans*

Yi-Ming Li, Gary Franklin, Heng-Mi Cui, Kristian Svensson, Xiao-Bing He, Gail Adam, Rolf Ohlsson and Susan Pfeifer

J. Biol. Chem. 1998, 273:28247-28252.
doi: 10.1074/jbc.273.43.28247
